



Article

NO_x Emission of a Correlation between the PEMS and SEMS over Different Test Modes and Real Driving Emission

Young Soo Yu ^{1,2}, Jun Woo Jeong ^{1,3}, Mun Soo Chon ¹ and Junepyo Cha ^{1,*}

¹ Department of Automotive Engineering, Korea National University of Transportation, Chungju 27469, Korea; yys1515@ut.ac.kr (Y.S.Y.); jjw112@ut.ac.kr (J.W.J.); mschon@ut.ac.kr (M.S.C.)

² Department of Mechanical Convergence Engineering, Graduate School of Hanyang University, 222 Wangsimni-ro, Seongdong-gu, Seoul 04763, Korea

³ Department of Mechanical Engineering, Hanyang University, Seoul 426-791, Korea

* Correspondence: chaj@ut.ac.kr

Abstract: The aim of this study is to verify the reliability of NO_x emissions measured using Smart Emissions Measurement System (SEMS) equipment in comparison with the NO_x emissions measured using certified Portable Emissions Measurement System (PEMS) equipment. The SEMS equipment is simple system, and it is less expensive than the PEMS equipment, as it comprises an On-Board Diagnostics (OBD) signal from the test vehicle and a NO_x sensor. The SEMS equipment based on low-cost sensors has an advantage of building big data, but there are insufficient previous studies comparing of NO_x emissions with certified the PEMS equipment. Therefore, this study is important in verifying the suitability of the SEMS equipment by comparing the NO_x emissions measured by the various test modes and RDE using the two types of equipment. To analyze the correlation between the PEMS and SEMS equipment, the advanced diesel vehicle was equipped with the two types of equipment to simultaneously measure NO_x emissions. After installing the equipment on the test vehicle, it was conducted under various test modes in the laboratory and the Real Driving Emission (RDE) test to verify the correlation of NO_x emissions measured by the SEMS equipment. The correlation analysis for the NO_x emissions measured by the PEMS and SEMS equipment under various test conditions and the RDE test indicated that the slope of the NO_x emissions was approximately equal to 1, and the coefficient of determination was 0.9 or higher. Based on these test results, it was concluded that NO_x emissions measured by the PEMS and SEMS equipment are highly similar.

Keywords: worldwide harmonized light-duty vehicle test cycle; real driving emissions; portable emissions measurement system; smart emissions measurement system



Citation: Yu, Y.S.; Jeong, J.W.; Chon, M.S.; Cha, J. NO_x Emission of a Correlation between the PEMS and SEMS over Different Test Modes and Real Driving Emission. *Energies* **2021**, *14*, 7250. <https://doi.org/10.3390/en14217250>

Academic Editors: Sergio Ulgiati and Evangelos G. Giakoumis

Received: 9 August 2021

Accepted: 1 November 2021

Published: 3 November 2021

Publisher's Note: MDPI stays neutral with regard to jurisdictional claims in published maps and institutional affiliations.



Copyright: © 2021 by the authors. Licensee MDPI, Basel, Switzerland. This article is an open access article distributed under the terms and conditions of the Creative Commons Attribution (CC BY) license (<https://creativecommons.org/licenses/by/4.0/>).

1. Introduction

Since September 2017, Republic of Korea and Europe have introduced Real Driving Emission Light-Duty Vehicle (RDE-LDV) test to strengthen the emission regulations for light-duty diesel vehicles [1]. The RDE-LDV test was introduced to address the defeat device, which arbitrarily manipulates the vehicle's Engine Control Unit (ECU) program when driving on the real road. When the RDE-LDV test was first introduced in September 2017, it was regulated such that the Euro 6b regulation with the Conformity Factor (CF) of 2.1 during the RDE test. In addition, the Euro 6d-temp regulation with the CF should be 1.5 times from 2019. Furthermore, the CF will finalize as 1.43 by January 2020 [2,3]. The CF means the Not To Exceed (NTE) for the respective pollutants such as NO_x, PN, and is the ratio of exhaust emitted during RDE against the regulatory standards of the vehicle [4].

Currently, the RDE-LDV test has been regulated to be measured by the Portable Emission Measurement System (PEMS, Sensors Inc., Saline, MI, USA). The PEMS equipment must be installed outside the vehicle, as illustrated in Figure 1. However, it faces challenges relating to the operation of complex equipment, the large size of the equipment,

and cost of test operations [5]. The expensive PEMS equipment is able to measure several emission components, but it is difficult to build big data of air pollution monitoring research on vehicles. To address these challenges, Nederlandse Organisatie voor toegepast-natuurwetenschappelijk onderzoek (TNO) developed the Smart Emissions Measurement System (SEMS, TNO, Den Haag, The Netherlands) equipment based on low-cost sensors and vehicle On-Board Diagnostics (OBD) data. Several studies have extensively investigated the SEMS equipment [6–12]. As an example, the TNO reported that a correlation test was conducted to simultaneously measure the exhaust emissions with the SEMS equipment and the Constant Volume Sampler (CVS) equipment under laboratory test modes such as the New European Driving Cycle (NEDC), World-wide harmonized Light-duty vehicles Test Cycles (WLTC) and Common Artemis Driving Cycles (CADC). Based on the reported results, the error in CO₂ measurements between the SEMS and CVS equipment was 0.3%, whereas the error in NO_x was 8.8%. These results confirmed that the CO₂ and NO_x data measured by the SEMS equipment exhibit high reliability [13]. Heepen et al. [14] presented an introduction of the difference between PEMS and SEMS equipment. In addition, this paper will give the measurement results and the functional features over long periods of time in the SEMS equipment. Vermeulen et al. [15] presented tail-pipe emissions of vehicles with Euro VI engines that were examined using the SEMS equipment under real-world conditions. To check the data measured by the SEMS equipment, the PEMS equipment has been used to measure the NO_x emissions on the public road. However, the PEMS and SEMS equipment were not operated simultaneously.



Figure 1. Example of the PEMS equipment installed on the test vehicle.

As mentioned above, little is known about previous studies that simultaneously measure NO_x emissions under various test modes and RDE using the two types of equipment. Therefore, to confirm data reliability, this study compared NO_x emissions measured by the SEMS equipment in various test modes, on a chassis dynamometer, in a laboratory with NO_x emissions measured by the PEMS equipment. After the reliability of NO_x emissions measured by the SEMS equipment was verified, the advanced diesel vehicle, which meets Euro 6d-temp regulations was equipped with the PEMS and SEMS equipment to measure data from a driving route that satisfies the trip requirements suggested by European Commission-Joint Research Centre (EC-JRC). The details on the trip requirements are introduced in Section 2.3.2.

The purpose of this study is to simultaneously measure NO_x emissions using PEMS and SEMS equipment on various real driving routes, considering the driving conditions in South Korea. This study attempts to verify the reliability of NO_x emissions measured by the SEMS equipment by comparing the results with NO_x emissions measured by the certified PEMS equipment.

Finally, after the operation based on the chassis dynamometer and Real Driving Emission (RDE) test, this study intends to apply the emission gas measurement system via the simplified SEMS equipment, instead of the complicated and the expensive PEMS equipment.

2. Experimental Method

2.1. Chassis Dynamometer and Exhaust Emission Analysis System

To evaluate the various test modes on the chassis dynamometer, it is necessary to understand the chassis dynamometer and exhaust analyzer. To simulate the real driving conditions, a unique resistance value for the test vehicle needs to be input to the dynamometer system. Driving along the entered driving mode such as NEDC and WLTC, exhaust emissions occur from the test vehicle. Then, the exhaust emissions from the test vehicle were consistently collected using CVS equipment. The exhaust emissions were analyzed by appropriately diluting the air using an exhaust analyzer.

Figure 2 presents a schematic of the chassis dynamometer in the laboratory and illustrates an example for the correlation test of the PEMS, SEMS, and CVS equipment. Furthermore, the specifications of the chassis dynamometer and exhaust emissions analyzer are summarized in Tables 1 and 2.

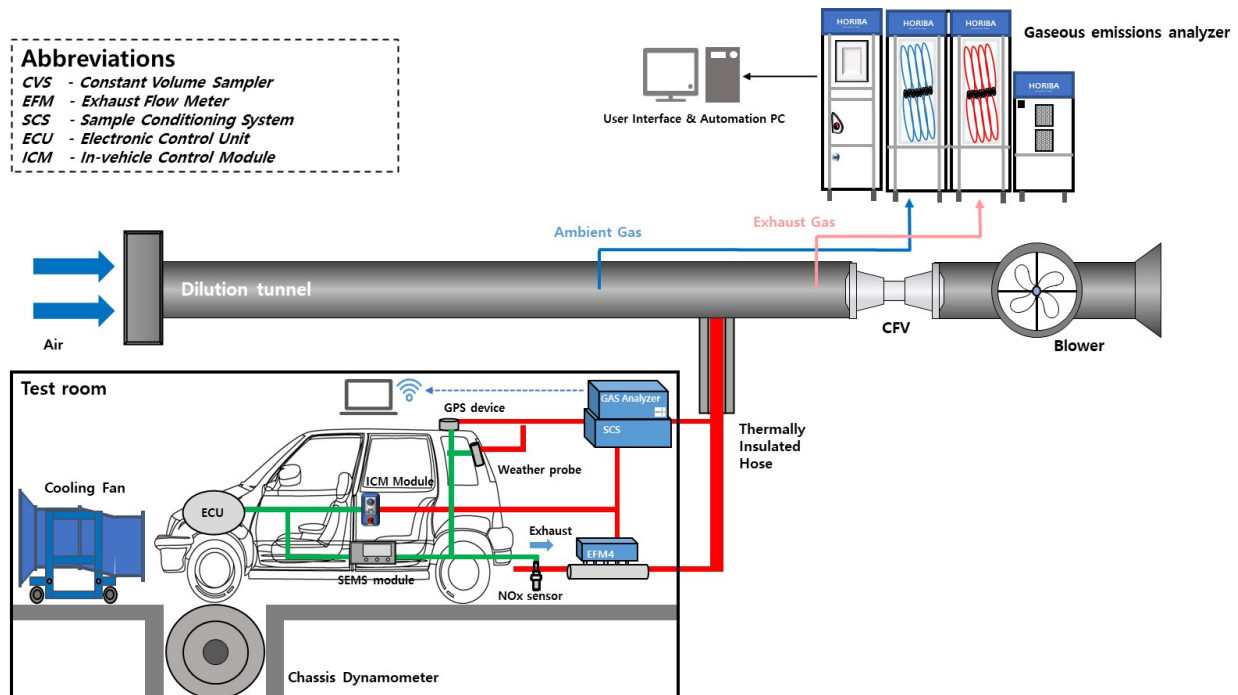


Figure 2. Schematic diagram of correlation test between the PEMS and laboratory exhaust emission analyzer.

Table 1. Specifications of chassis dynamometer.

Item	AVL
Roller	Single Roll 48 inch (MIM type)
Inertia weight range (kg)	454–5448
Maximum roll speed (km/h)	200
Electric motor absorber type	AC motor
Speed deviation	±0.1% F.S.
Torque deviation	±0.02 km/h
Driving distance measurement	Encoder
Cooling fan	Variable speed

Table 2. Specifications of exhaust emission analyzer.

Item	HORIBA
Constant volume sampler	CVS-7400T
Motor exhaust gas analyzer	MEXA-7200H
Dilution tunnel sampler	DLS-7100E
Dilution tunnel	DLT-1230

2.2. Various Test Modes in Laboratory

To analyze the correlation between NO_x emissions measured by PEMS and SEMS equipment, this study performed various test modes on a chassis dynamometer in the laboratory. The test modes were conducted over six different chassis dynamometer modes: the NEDC; the WLTC, which reflects realistic trip conditions than the NEDC mode; the Federal Test Procedure-75 (FTP-75) mode, which is known as the representative urban driving conditions of USA; the Highway Fuel Economy Test (HWFET), which is reflecting the highway driving conditions of USA; the US06, which is an aggressive high speed and high load driving mode; the SC03, which operates the air conditioner to reflect summer environmental conditions. In addition, the driving characteristics of the test mode in this study are shown in Table 3.

Table 3. Summaries of test modes in laboratory.

Item	NEDC	WLTC	FTP-75	HWFET	US06	SC03
Trip duration (s)	1180	1800	1874	765	594	594
Trip distance (km)	11.03	23.27	17.77	16.45	12.87	5.79
Avg. vehicle speed (km/h)	33.6	46.5	34.1	77.7	77.9	34.1
Maximum acceleration (m/s ²)	1.04	1.67	1.48	1.43	3.79	2.28
Engine start condition	Cold Warm	Cold Warm	Cold	Warm	Warm	Warm

2.2.1. Test Vehicle and After-Treatment System

The test vehicle in this study is an SUV-type diesel vehicle (Hyundai motor group, Seoul, Korea) equipped with combination of Lean NO_x Trap (LNT), Diesel Particle Filter (DPF), and Selective Catalytic Reduction (SCR) to meet the Euro 6d-temp regulations. In addition, the test vehicle features sophisticated after-treatment technology. The specifications of the test vehicle are shown in Table 4.

Table 4. Specifications of test vehicle [10].

	Vehicle 01
Type	SUV
Maximum power kW	137
Displacement cc	1995
Engine type	CRDI I4
Model year	2019
Emission regulation	Euro 6d-temp
After-treatment	LNT + DPF + SCR

2.2.2. RDE Route

The RDE-LDV test route should sequentially comprise an urban, a rural, and a motorway, in accordance with the trip requirements suggested by the European Union (EU). The trip distance of each part should be at least 16 km. In addition, the urban, rural, motorway parts should account for 34, 33%, and 33% of the total trip share. In particular, the urban part should include a minimum stop ratio of 6–30% among urban driving. In addition, the

total driving duration should lie between 90 and 120 min, and the difference in the route's altitude between the start and end points should be less than 100 m [4].

In this study, the RDE tests were performed along Route A and Route B developed by satisfying the above conditions. As illustrated in Figure 3a, Route A reflects driving patterns such as low vehicle traffic in urban areas of small and medium cities in Republic of Korea, and this route has a total distance of 93.3 km, including urban, rural, motorway parts. As illustrated in Figure 3b, Route B reflects the representative traffic density and comprises a highly populated metropolitan area (Seoul) in Republic of Korea. In addition, it is a route with a total distance of 70.5 km, including urban, rural, motorway parts. The major difference between Routes A and B is the vehicle speed according to the traffic jam in the urban part.

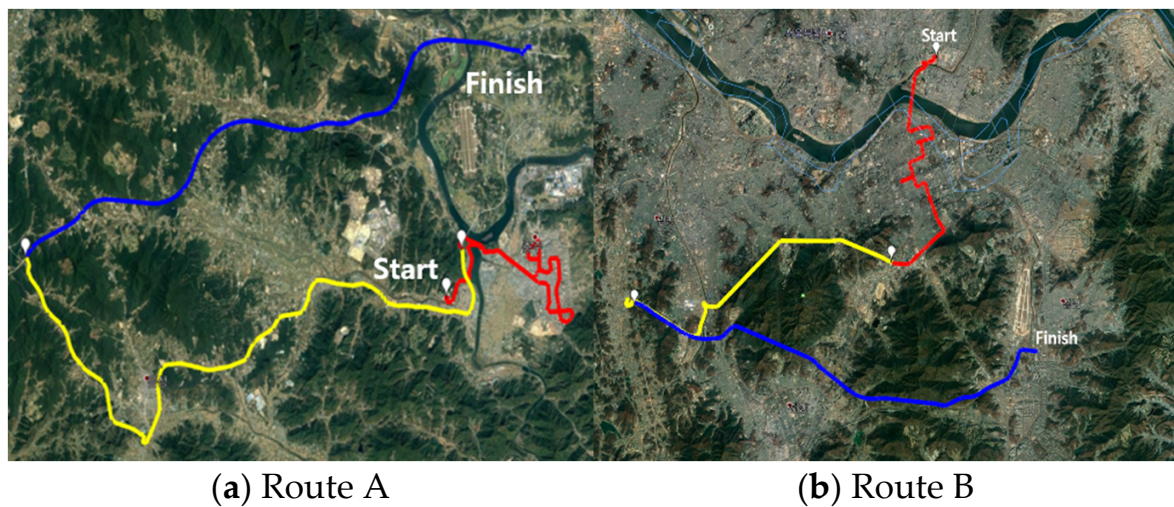


Figure 3. Map of RDE routes—Urban (redline), Rural (yellow line), Motorway (blue line).

As presented in Figure 4, it can be observed that Route B has more areas with vehicle speeds below 30 km/h than Route A. In areas where the vehicle speed is low, vehicle congestion is frequent; accordingly, this vehicle congestion triggers an increasing stop ratio in the urban part. Based on the RDE test, it can be confirmed, as shown in Table 5, that the stop ratio in the urban part of Route B was 36.39%, which is approximately 12% higher than that of Route A.

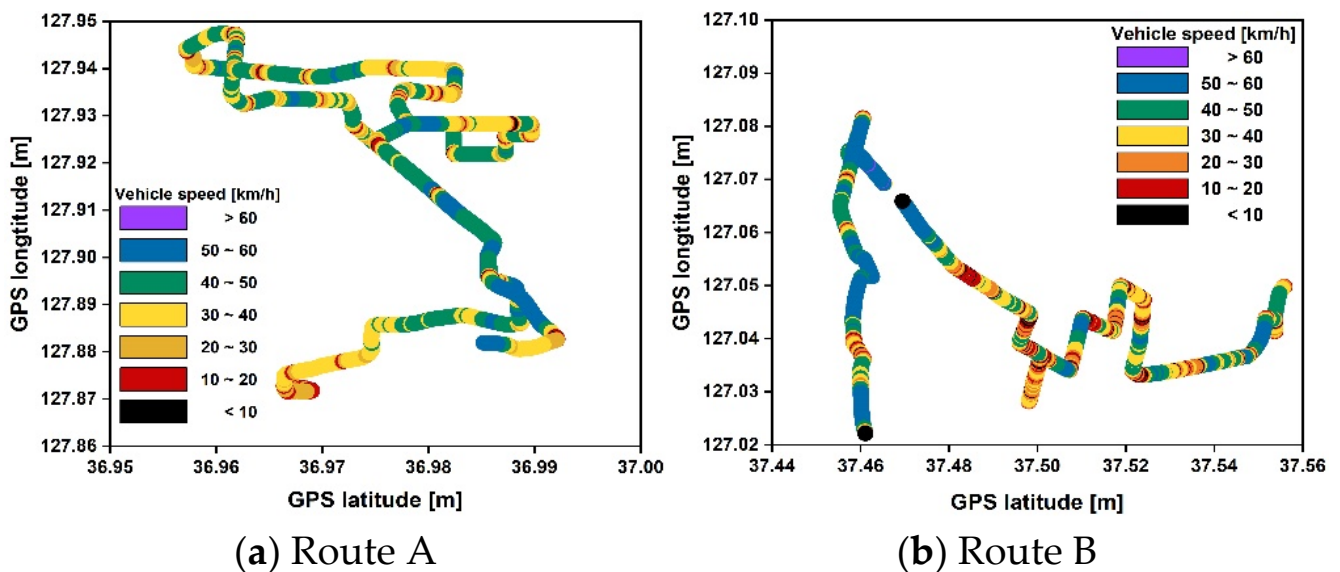


Figure 4. GPS location of urban in RDE routes; the color indicates the vehicle speed.

Table 5. Summaries of RDE test routes.

		Urban	Rural	Motorway	Total
Route A	Trip distance (km)	30.9	32.0	29.9	92.8
	Trip share (%)	31.3	36.7	32.1	100.0
	Trip duration (min)	78.4	25.0	14.6	119.8
	Average vehicle speed (km/h)	26.4	77.6	107.9	
Route characteristics: stop duration of urban part is 23.79%					
Route B	Trip distance (km)	22.0	23.0	21.4	66.4
	Trip share (%)	33.1	34.7	32.2	100.0
	Trip duration (min)	59.1	17.5	13.9	90.5
	Average vehicle speed (km/h)	17.6	76.5	117.3	
Route characteristics: stop duration of urban part is 36.37%					

Finally, RDE tests were performed several times on the test vehicle at each driving route, and the detailed characteristics of the driving routes are summarized in Table 5.

2.3. Test Equipment

2.3.1. The PEMS Equipment

The PEMS equipment considered in this study was obtained from the SEMTECH-LDV corporation (Sensor Inc., Saline, MI, USA). The PEMS equipment comprise an exhaust gas analyzer, an exhaust gas flow meter, a GPS device, a weather probe with ambient gas and pressure, a power supply device, and an OBD data acquisition device.

The PEMS equipment measure emission concentration data (ppm) at 1 Hz. Then, the emission concentration data (ppm) are synchronized with the flow rate of the exhaust flow meter and converted to the exhaust mass data (g/s). In addition, exhaust mass data (g/s) are synchronized with the vehicle speed (km/h) measured in GPS and OBD devices and converted to emissions per mileage (g/km).

The exhaust emissions measured by the principle of Pitot tube in the exhaust flow meter were measured and analyzed by the exhaust gas analyzer inside the PEMS equipment. Specially, NO and NO_x emissions were measured via the Non-dispersive ultraviolet (NDUV) principle, while CO and CO₂ emissions were measured via the Non-dispersive infrared (NDIR) principle. The detailed specifications and principles of the PEMS equipment are summarized in Table 6.

Table 6. Specifications of PEMS equipment [10].

Principle	Specifications
Heated NDIR	CO: 0–8% vol. CO ₂ : 0–18% vol.
Heated NDUV	NO: 0–3000 ppm NO ₂ : 0–1000 ppm
Operating temperature (°C)	–10–45
Tolerance of CO, CO ₂ , NO, NO ₂ emissions	±2%
Dimensions (mm)	SCS module: 435(W) × 410(D) × 105(H) GAS module: 437(W) × 312(D) × 135(H) EFM module: 365(W) × 105(D) × 90(H)
Weight (kg)	SCS module: 10.9 GAS module: 8.9 EFM module: 3.9

2.3.2. The SEMS Equipment

The SEMS equipment used to measure exhaust emissions from the test vehicle in this study comprise NO_x sensors, a GPS signal that measures vehicle speed and altitude of the driving route, an OBD signal that measures the OBD data of the test vehicle, the main

module that is responsible for the operation of the sensors, data storage, and power supply of the equipment.

The detailed specifications and measurement principle of the NO_x sensor are summarized in Table 7. The NO_x sensors were mounted on the exhaust pipe of the test vehicle, as illustrated in Figure 5. In addition, the mass flow rate of NO_x in the SEMS equipment was calculated using the concentration of NO_x in the exhaust pipe, and the exhaust mass flow rate was calculated based on the intake air flow rate and the fuel flow rate measured via the OBD data of the ECU program of the test vehicle.

Table 7. Specifications of NO_x sensor in SEMS equipment [10].

Principle	Specifications
Measurement	ZrO ₂ -based multi-layer sensor with integrated heater and three oxygen pumps
Output signals	NO _x , linear λ or O ₂ concentration
Electrical system (V)	12
Operating temperature (°C)	100–800
Principle	Amperometric
NO _x tolerance	0–100 ppm: ± 20 ppm 100–1500 ppm: $\pm 20\%$
Measuring range	NO _x : 0–1500 ppm λ : -0.994 – 1.010

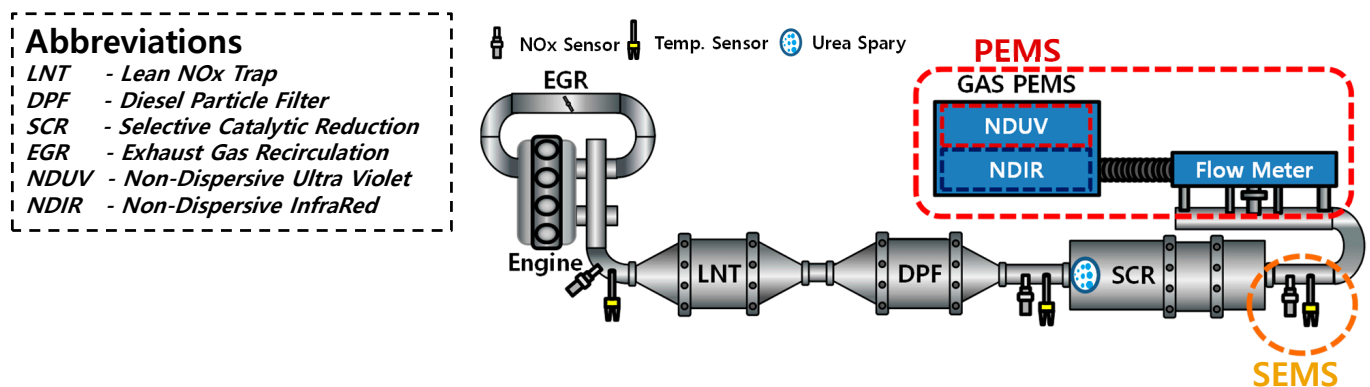


Figure 5. Schematic diagram of the PEMS and SEMS equipment installed on the test vehicle.

2.3.3. Principles of the PEMS and SEMS Equipment

NO_x measure principle of PEMS equipment used the NDUV method. In NDUV method, when the exhaust emissions were sampled in the PEMS equipment, the injected exhaust emissions were passed through two cells. One cell has ultraviolet (UV) rays and the other cell has nitrogen that does not react with exhaust emissions. Among the exhaust emissions, when NO_x emissions were injected in the PEMS equipment, NO_x emissions absorb UV wavelengths by reaction in one cell and no reaction occurs in the other cell. At this time, NO_x emissions were measured by the difference in UV rays generated from the two cells. In addition, the CO and CO₂ measure principles of the PEMS equipment used the NDIR method. The NDIR method is similar to the NDUV method. The NDIR method used infrared rays instead of UV rays.

NO_x measure principle of SEMS equipment used the amperometric method. In the amperometric method, the measured NO_x emissions among the exhaust emissions pass through the diffusion barrier and move to the first cell. The first cell removes O₂ close to 0 ppm. Then, when moving to the second cell, most of O₂ is removed. Thus, NO and NO₂ molecules are decomposed to measure O₂ [16–18]. However, unlike the PEMS equipment, NO emissions measured by the SEMS equipment were increased via the urea solution.

Here, the urea solution is injected to reduce NO_x emissions in the SCR system. In the SEMS equipment, urea solution is decomposed as shown in equation (1) to increase NO emissions. As mentioned above, the SEMS equipment can be easily measured due to low cost and simple installation, but the limitation of the SEMS equipment is that NO emissions measured by the urea solution were also measured.



2.4. Reliability Verification of Data Measured by the PEMS Equipment

To verify the reliability of data measured by the PEMS equipment before the RDE test, the correlation test was performed to simultaneously measure the exhaust emissions emitted from the test vehicle with the PEMS and CVS on the chassis dynamometer in the laboratory.

The correlation test was performed under various test modes. The results obtained from the correlation test measurements are summarized in Figure 6. In addition, the schematic of the correlation test is presented in Figure 2. Owing to the comparison with data measured by the PEMS and CVS equipment, the slopes for NO_x and CO₂ corresponded to 1.08 and 1.03, respectively. Accordingly, it was confirmed that the data measured by the PEMS equipment has high reliability.

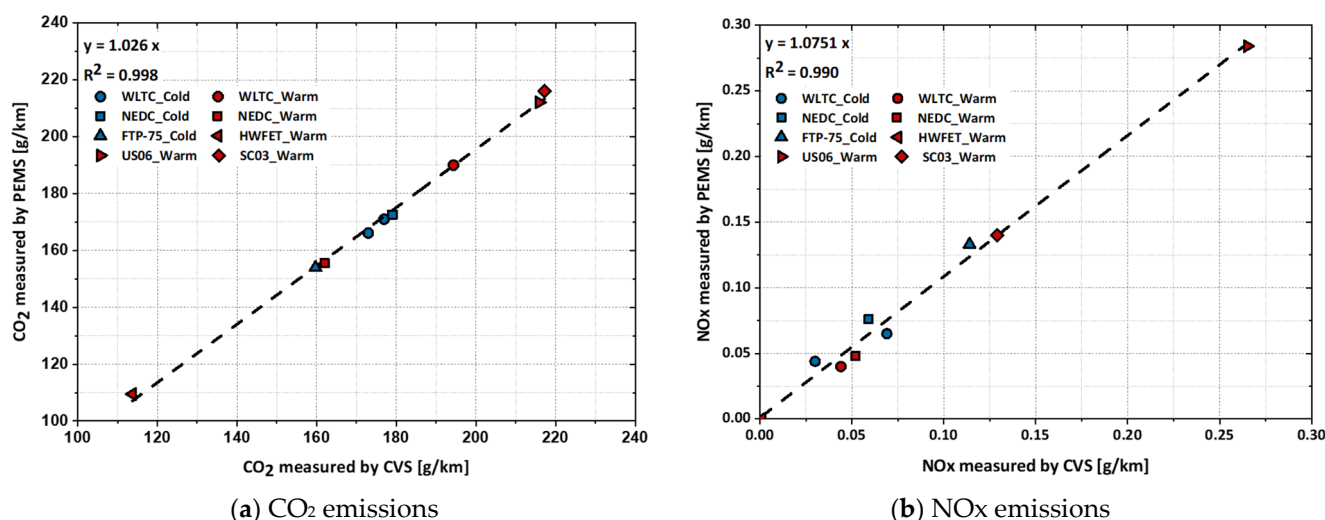


Figure 6. Comparison of exhaust emissions measured with the CVS and PEMS equipment.

2.5. Reliability Verification of Data Measured by the SEMS Equipment

Unlike the PEMS equipment, the SEMS equipment does not have an exhaust flow meter. Hence, mass air flow and total injection quantity from the OBD data of the test vehicle are introduced to calculate the exhaust flow rate. The calculated exhaust flow rate is used to convert the NO_x measured in concentration units (ppm) into mass units (g/s), as expressed in the following Equation (2) [4]. To verify the reliability of the SEMS equipment data, the exhaust flow rate measured by the exhaust flow meter of the PEMS equipment, and the exhaust flow rate calculated by introducing mass air flow and total injection quantity of the aforementioned OBD data are compared and presented in Figure 7.

$$m_{gas} = \rho_{gas} \times c_{gas} \times Q_{exh} \quad (2)$$

where:

- m_{gas} (g/s): the mass of the exhaust component “gas”;
- ρ_{gas} (kg/m³): the density of the exhaust component “gas”;
- c_{gas} (ppm): the concentration of the exhaust component “gas”;
- Q_{exh} (kg/s): the exhaust mass flow rate.

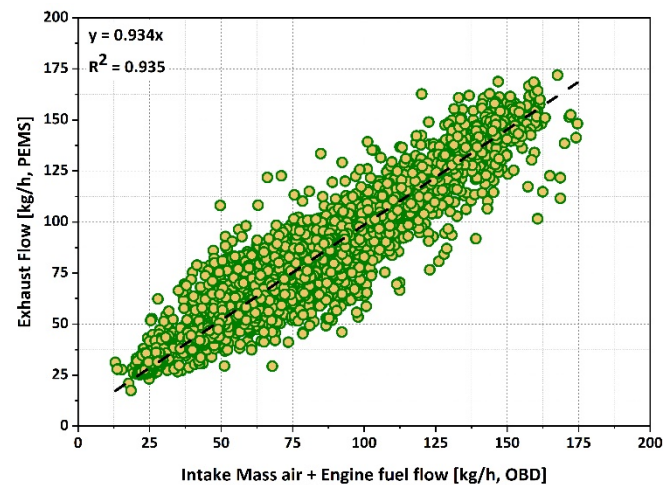


Figure 7. Correlation of exhaust flow measured by the PEMS and SEMS equipment.

In addition, the vehicle speed measured by GPS signal of the PEMS equipment and the vehicle speed measured by OBD data of the SEMS equipment are compared and presented in Figure 8. The comparison results indicated that the slope of the exhaust flow rate between the two types of equipment was 0.93, and the slope of the vehicle speed was significantly close to 1. Accordingly, it was possible to verify the reliability of the OBD data measured by the SEMS equipment.

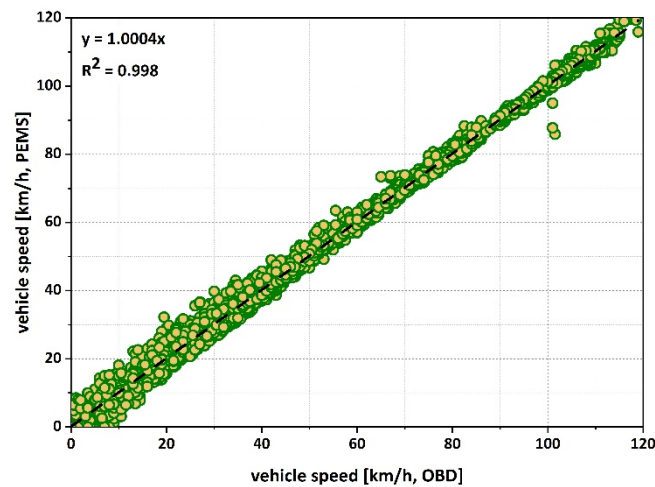


Figure 8. Correlation of vehicle speed measured by the PEMS and SEMS equipment.

3. Results

3.1. Correlation of NO_x Emissions between the PEMS and SEMS Equipment in Laboratory

In this study, the reliability of the NO_x emissions measured by the SEMS equipment was verified by comparing the results with the NO_x emissions measured by the PEMS equipment, which was verified through correlation with the CVS equipment in a laboratory.

Various test modes were considered for the test vehicle with the chassis dynamometer in the laboratory to verify the reliability of the SEMS equipment. The test results of the exhaust emissions from the test vehicle under the cold and hot conditions for each test mode are shown in Figure 9.

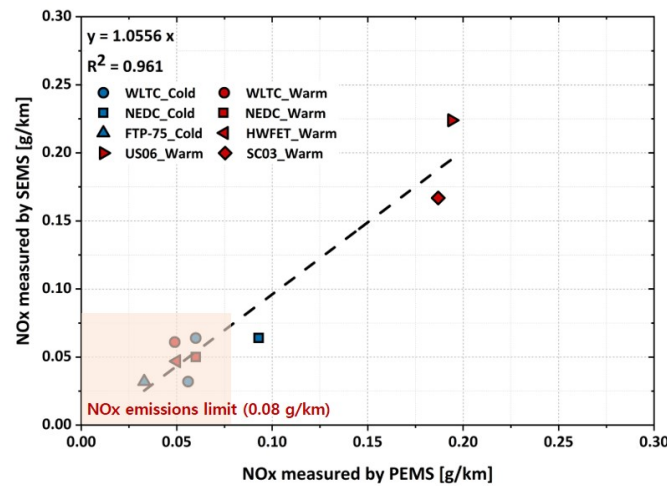


Figure 9. Correlation of NOx emissions measured by the PEMS and SEMS equipment under various test modes in the laboratory.

A total of nine correlation tests were conducted on a chassis dynamometer in the laboratory, and most of the NOx emissions measured by the PEMS and SEMS equipment were within the current NOx emission limit (0.08 g/km). In addition, it was verified that the slope of the NOx emissions measured by the PEMS and SEMS equipment exhibited a very close linearity to 1; the coefficient of determination was 0.961, thus indicating that the results were significantly similar.

Figure 10 presents a quantitative plot of NOx emissions measured by the PEMS and SEMS equipment. In phase 3 of the WLTC mode, NOx emissions measured by the SEMS equipment were significantly lower. Consequently, NOx emissions were measured close to zero. This is an error that cannot be measured over a range, which indicates significantly lower NOx emissions measured by the SEMS equipment. Thus, a measurement error of the NOx sensor may exist.

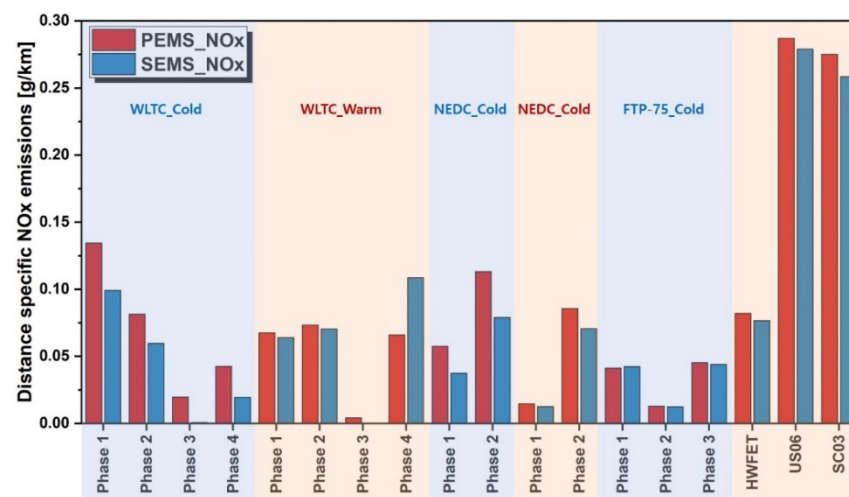


Figure 10. NOx emissions measured by the PEMS and SEMS equipment under various test modes in the laboratory.

Based on the testing under cold and hot conditions in the NEDC and WLTC modes, more NOx emissions were measured under the cold condition than of the hot condition. This is because excessive exhaust emissions are triggered by incomplete combustion owing to the low temperature in the combustion chamber of the engine at an initial start-up condition, and the catalyst of the after-treatment is not sufficiently preheated, thereby resulting in excessive exhaust emissions owing to low conversion efficiency [19,20].

Unlike the results of the other test modes, US06 and SC03 exhibited high NO_x emissions. As can be deduced from Table 3, the US06 mode is significantly more aggressive than other test modes, such as in its acceleration and driving characteristics. In the case of the SC03 mode, NO_x emissions are significantly high because it operates an air conditioner. If the air conditioner is operated, the engine in the test vehicle exerts an excessive load; hence, it is considered that NO_x emissions are substantially high.

Figure 11 presents the time continuous NO_x emissions measured by the PEMS and SEMS equipment under each test mode. It can be seen that profiles of NO_x emissions measured by the PEMS and SEMS equipment follow similarly under all the test modes.

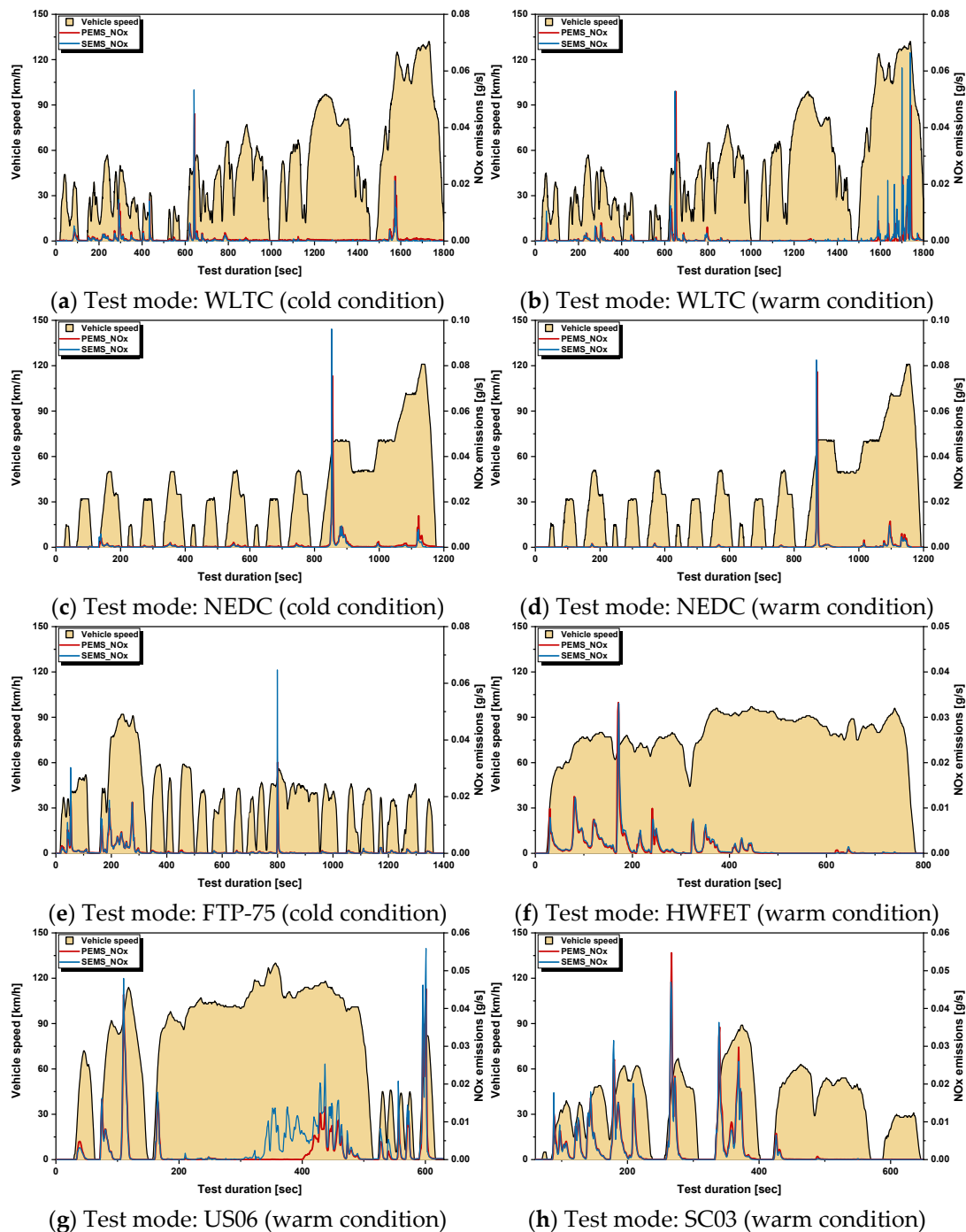


Figure 11. Real-time profiles of NO_x emissions measured by the PEMS and SEMS equipment under various test modes in the laboratory.

Based on the comparison of the NO_x emissions measured by the PEMS and SEMS equipment under various test modes on a chassis dynamometer in the laboratory, profiles of NO_x emissions measured by the PEMS and SEMS equipment follow similarly; this is because a laboratory test involves relatively fewer variables such as road grade and sharp acceleration and deceleration of dynamic conditions, as compared to real driving conditions. However, there was the difference that could not be measured by the SEMS equipment owing to the significantly low NO_x emissions in the section where the test vehicle was stabilized in the driving mode, such as phase 3 of the WLTC mode. This challenge is owing to the limitation of the low-cost NO_x sensor. The detailed limitation of NO_x sensor means NO_x tolerance. The tolerance of NO_x sensor is ± 20 ppm measured within 0~100 ppm. There is a limit due to NO_x tolerance when measured as low as 20 ppm or less. Therefore, it was confirmed that future technology development is required.

3.2. Detailed Analysis on Real-Time Profiles of NO_x Emissions for Characteristics of the NO_x Conversion in Laboratory

As shown in Figure 11, it can be observed that NO_x emissions measured by the PEMS and SEMS equipment agree well due to strong acceleration and high speed of vehicle under the various test modes. To analyze these results, the data measured in US06, which reflects the effect of acceleration and the data measured in HWFET mode and considers high speed driving, are comprehensively presented, as illustrated in Figures 12 and 13.

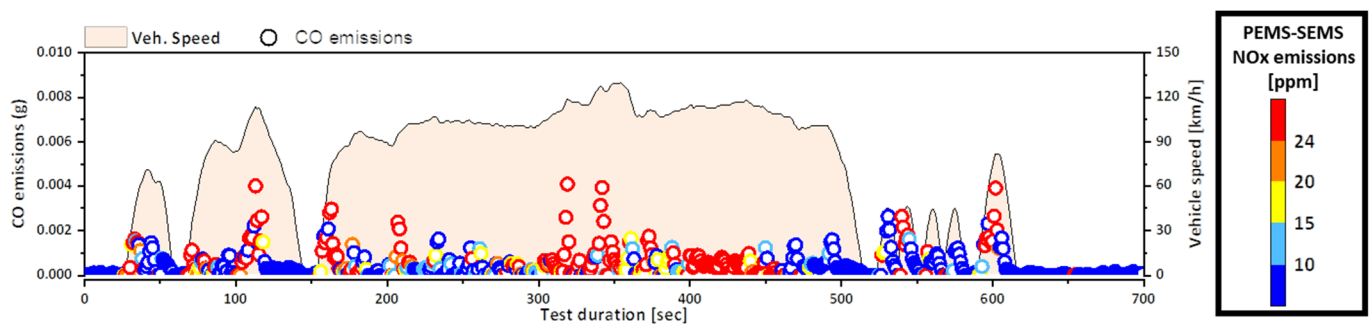


Figure 12. Real-time profiles of CO emissions and the difference between NO_x emissions measured by the PEMS and SEMS equipment under US06 test modes in the laboratory.

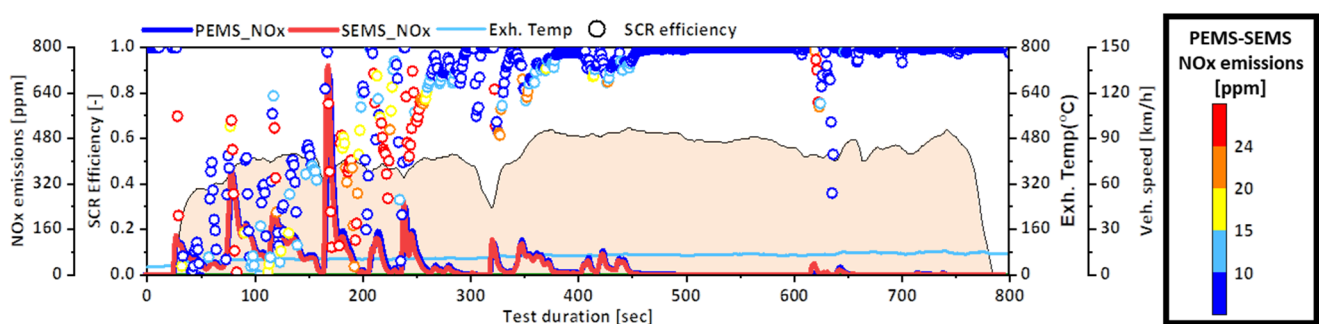


Figure 13. Real-time profiles of SCR efficiency and the difference between NO_x emissions measured by the PEMS and SEMS equipment under HWFET test modes in the laboratory.

Figure 12 presents the measured data of the US06 mode, which reflects acceleration conditions, among the various modes on the chassis dynamometer in the aforementioned laboratory in real time. The analysis indicated that the difference between the NO_x emissions measured by the PEMS and SEMS equipment was large because of the increase in CO emissions during acceleration. This is ascertained to be the effect of the LNT system installed on the test vehicle. The LNT system is a catalyst that reduces NO_x emissions

without a reducing agent, such as NH_3 . In addition, the LNT catalysts run periodically under lean (oxidizing) and rich (reducing) conditions [21].

Figure 14 illustrates the principle of the LNT system under lean and rich conditions, and there is a detailed explanation of the NO_x storage and reduction behavior.

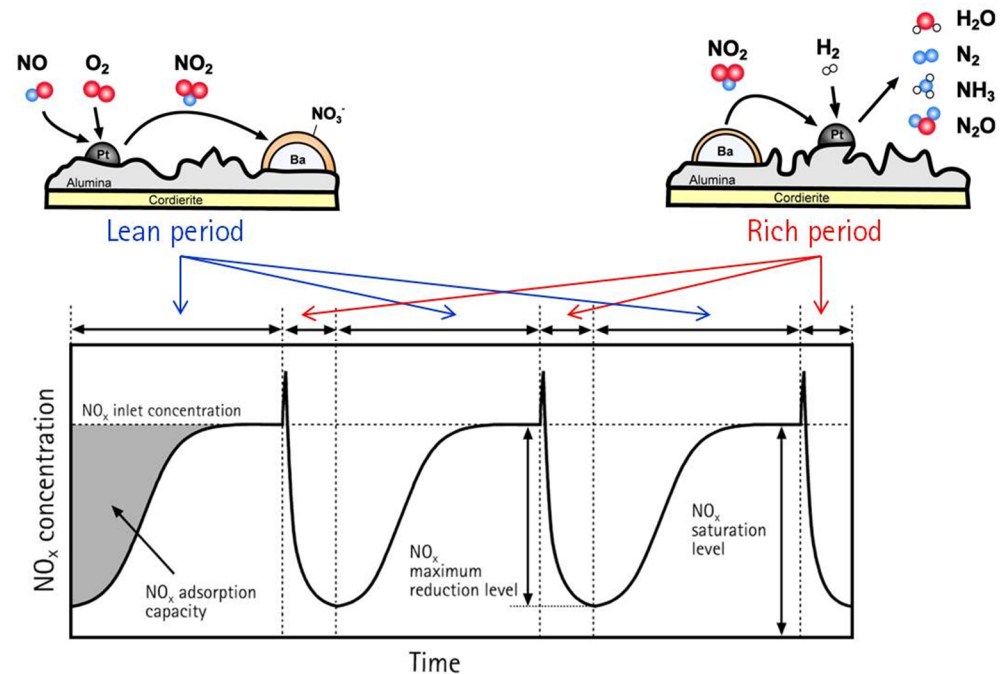


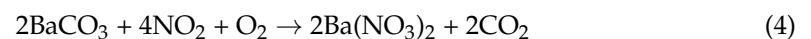
Figure 14. Schematic of the LNT system mechanism.

The first step is that the NO emissions were oxidized to NO_2 under lean conditions, as expressed in Equation (3). Then, the NO_2 emissions react with oxygen in the LNT system to reduce nitrogen oxides and generate carbon dioxide, as expressed in Equation (4). To reduce NO_x emissions, CO and HC in the exhaust gases are applied as reducing agents or post-injections. The last step involves the oxidation and reduction of NO_x emissions, which are converted to NO and CO_2 , as expressed in Equation (5) [22,23].

Oxidation of NO , and formation of NO_2 (lean conditions)



Absorption of NO_x inside the LNT system (lean conditions)



Release of the stored NO_x from the LNT system surface (rich conditions)

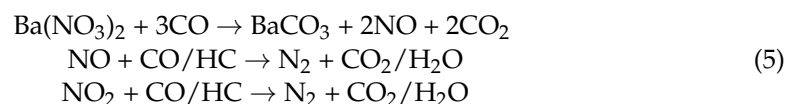


Figure 13 illustrates the difference between the NO_x emissions measured by the two equipment types in real time according to the NO_x conversion efficiency of the SCR system in the HWFET mode, which simulates highway driving.

Based on the analysis, it was confirmed that when the NO_x conversion efficiency of the SCR system decreases, the difference between the NO_x emissions measured using the two types of equipment increases. These results need to be determined based on the SCR

system. Figure 15 presents the schematic of the SCR mechanism. The NO_x reduction effect of the SCR catalyst is expressed as follows in Equations (6)–(8) [24,25].

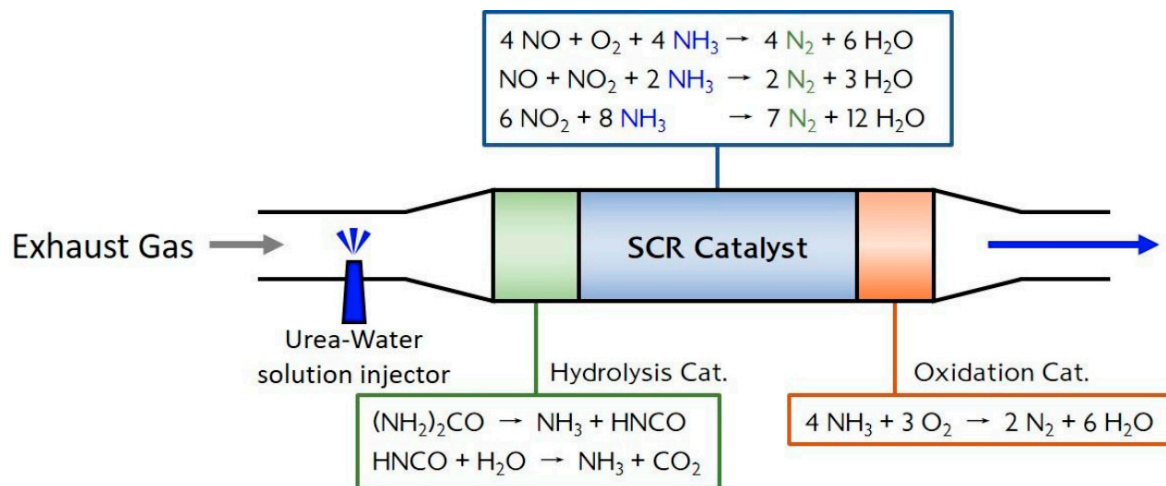
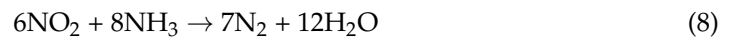
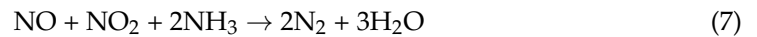
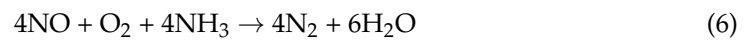
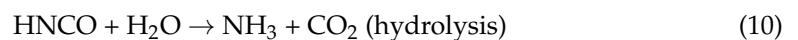
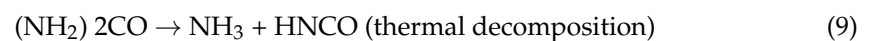


Figure 15. Schematic of the SCR system mechanism.

In the above equation, NH₃ does not react with oxygen under normal exhaust temperatures below 550 °C; hence, the most significant NO_x reduction effect of SCR is 100%.

Urea solution is supplied before the SCR system, and is hydrolyzed to NH₃ via two steps of the following Equations (9) and (10) by the intermediate product isocyanic acid under an exhaust temperature above 250 °C [26].



The NO_x conversion is sensitive to temperature, and hydrolysis does not occur even if excess urea solution is injected under low temperatures. Therefore, the NO_x conversion is possible, using the absorbed NH₃ of the urea solution. However, if the temperature increases rapidly, the absorbed NH₃ is released and oxidized on reacting with oxygen. Then, the NO_x conversion decreases as much as the excessive NH₃ [27].

Therefore, the urban part with frequent acceleration is expected to have higher NO_x emissions measured by the PEMS and SEMS equipment under the effect of the LNT system, as compared to other parts. Although, in the motorway part, NO_x emissions are significantly reduced by chemical reactions with NH₃ inside the SCR system, it is expected that NH₃ is excessively injected, thereby resulting in a difference between NO_x emissions measured by PEMS and SEMS equipment. As the NO_x sensor installed in the SEMS equipment measures NO and NO₂ emissions from NO_x and NH₃ emissions, it cannot measure only NO_x emissions. The details on the information are introduced in Section 2.3.3. Hence, in the motorway part, it is expected that NO_x emissions measured by the SEMS equipment will be higher than the NO_x emissions measured by the PEMS equipment.

3.3. Correlation of NO_x Emissions between the PEMS and SEMS Equipment On-Road

In this study, NO_x emissions were measured by the PEMS and SEMS equipment over a total of 33 (Route A = 30 times, Route B = 3 times) on-road conditions with various driving variables compared to the various test modes, on a chassis dynamometer in the laboratory.

In Figure 16, the red circles indicate NO_x emissions measured by PEMS and SEMS equipment on Route A, and the blue circles indicate NO_x emissions measured by PEMS and SEMS equipment on Route B. Based on the comparison of NO_x emissions measured by PEMS and SEMS equipment under RDE tests, the slope of the RDE test was 0.816, which is lower than the slope of the laboratory test. The slope of the RDE test was lower than that of the chassis dynamometer because the test was considered owing to the various on-road driving variables, such as a traffic jam in the urban part, driving style according to the driver, and road grade of route. These various on-road driving variables affect the engine load of vehicle. As the engine load of the vehicle increases, NO_x emissions increase, and the tolerance of NO_x emissions measured by the two types of equipment increases [28]. For this reason, the slope of the on-road is lower than that of the chassis dynamometer. In addition, the coefficient of determination was 0.922, thus indicating that the results were very similar. Most of the test results were within the RDE NO_x emissions limit (0.1144 g/km).

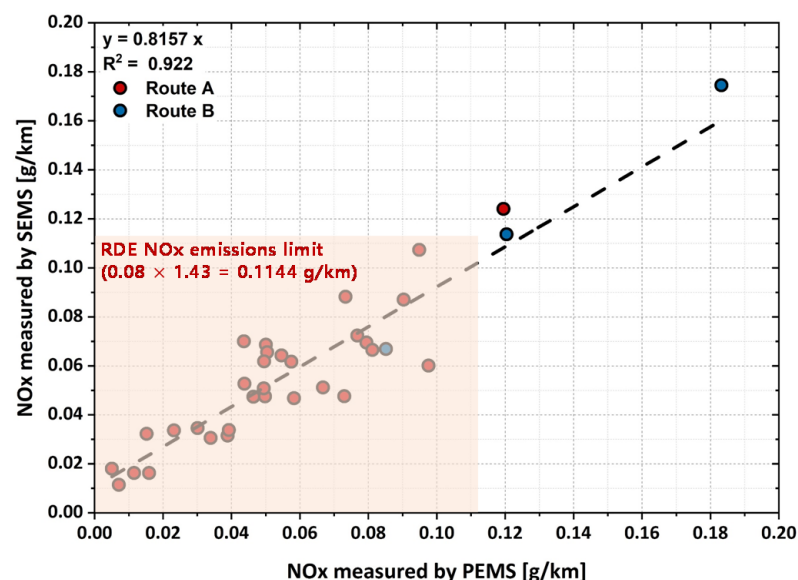
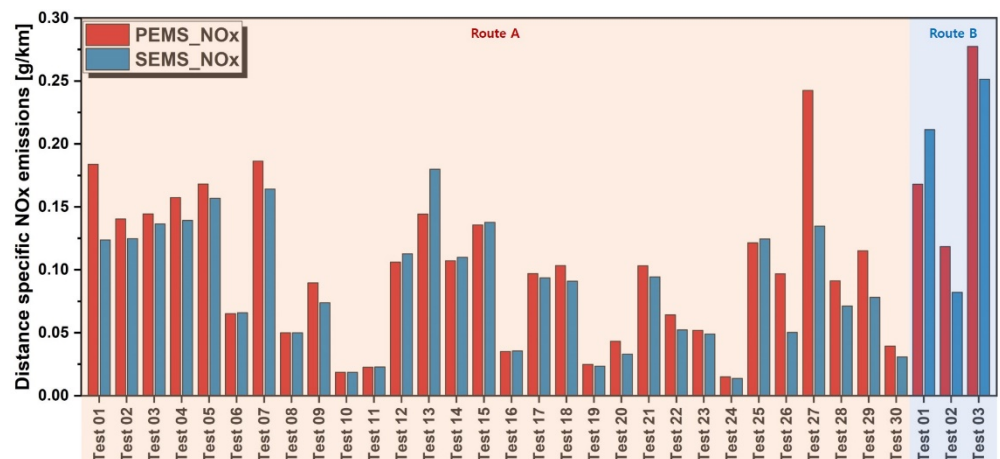
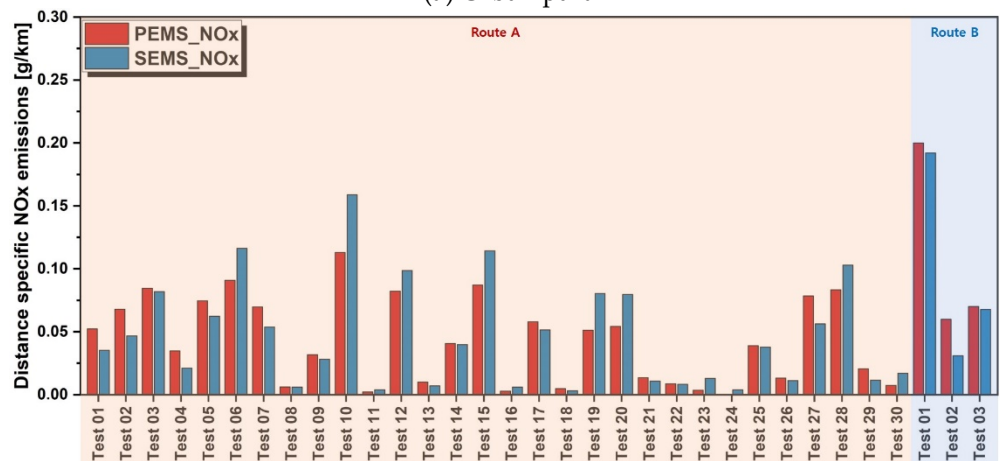


Figure 16. Correlation of NO_x emissions measured by the PEMS and SEMS equipment under RDE tests in Routes A and B.

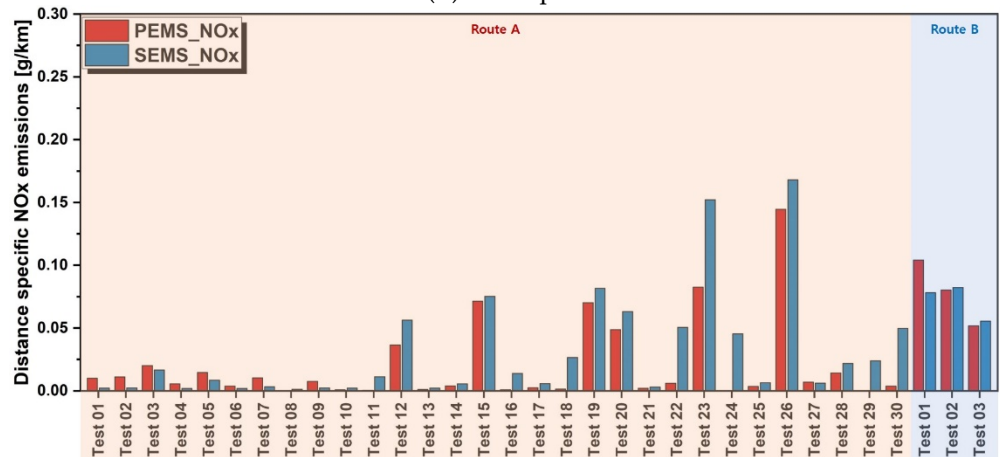
As presented in Figure 17, NO_x emissions measured by PEMS and SEMS equipment on Routes A and B were quantitatively indicated for urban, rural, and motorway parts. Regarding the urban part, it was determined that NO_x emissions were higher than that of other driving parts because there were various driving characteristics such as vehicle congestion owing to the shutdown of the signal system, and a highly populated metropolitan area. Regarding the rural and motorway, it was determined that NO_x emissions were lower than that of the urban part because of inertia driving with a fuel-cut, which can improve the fuel efficiency of the vehicle, and reduced exhaust emissions becomes possible as vehicle speed increases [29]. In addition, NO_x emissions measured by the SEMS equipment were relatively higher than that of the PEMS equipment. As this is an amperometric method, it is based on the principle of the NO_x sensor in the SEMS equipment. The amperometric method generates nitrogen and oxygen by splitting NO_x (NO and NO₂), as defined in the following equations. At this point, the generated O₂ molecules are measured as the NO_x inside the sensor.



(a) Urban part



(b) Rural part



(c) Motorway part

Figure 17. NOx emissions measured by the PEMS and SEMS equipment under RDE tests in Routes A and B.

However, the NOx sensor adopted in this study measures NH₃ emissions, and the measured NH₃ emissions are split into NO and H₂O, owing to the chemical reaction [28]. As aforementioned, the split chemical equation of NH₃ emissions emerges accordingly.

Accordingly, it was determined that NOx emissions measured by the SEMS equipment were higher than those measured by the PEMS equipment.

Figures 18 and 19 illustrate real-time NOx emissions measured by PEMS and SEMS equipment for each driving part in Routes A and B, respectively. It can be observed

that the NO_x emissions measured by the PEMS and SEMS equipment under the RDE tests are similar. Unlike the results of the various test modes on a chassis dynamometer in the laboratory, NO_x emissions measured by the SEMS equipment were higher than those measured by the PEMS equipment because the RDE tests consider various driving variables. As mentioned above, excess NH₃ emissions from the SCR system, which adopts NH₃ as a reductant to reduce nitrogen oxides, were injected, such that it was determined that the NO_x emissions were measured by the NO_x sensor.

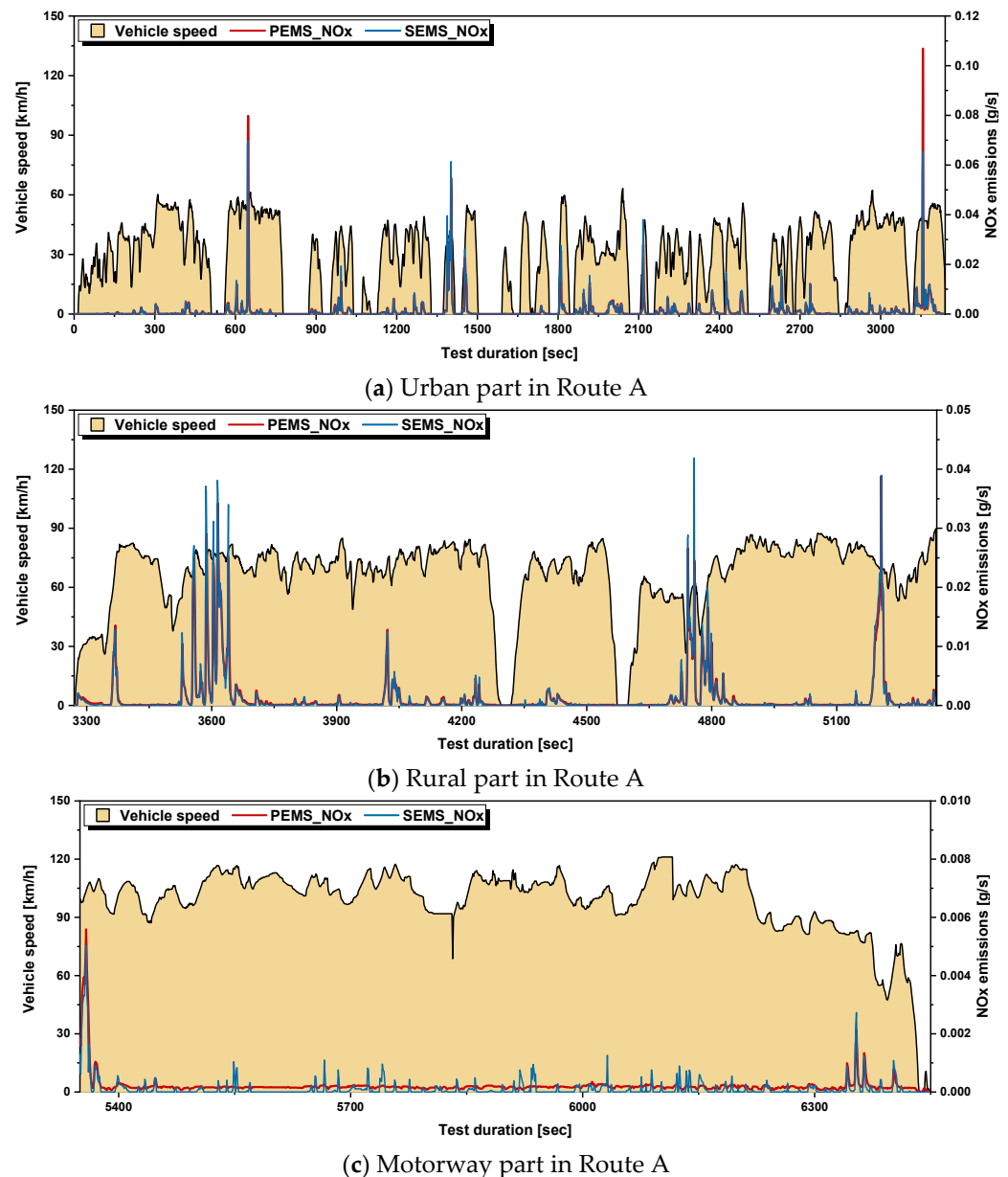


Figure 18. Real-time profiles of NO_x emissions measured by the PEMS and SEMS equipment under RDE Route A.

3.4. Detailed Analysis on Real-Time Profiles of NO_x Emissions for the Characteristics of the NO_x Conversion On-Road

Figures 20 and 21 present the differences between NO_x emissions measured by PEMS and SEMS equipment in urban and motorway part under RDE tests.

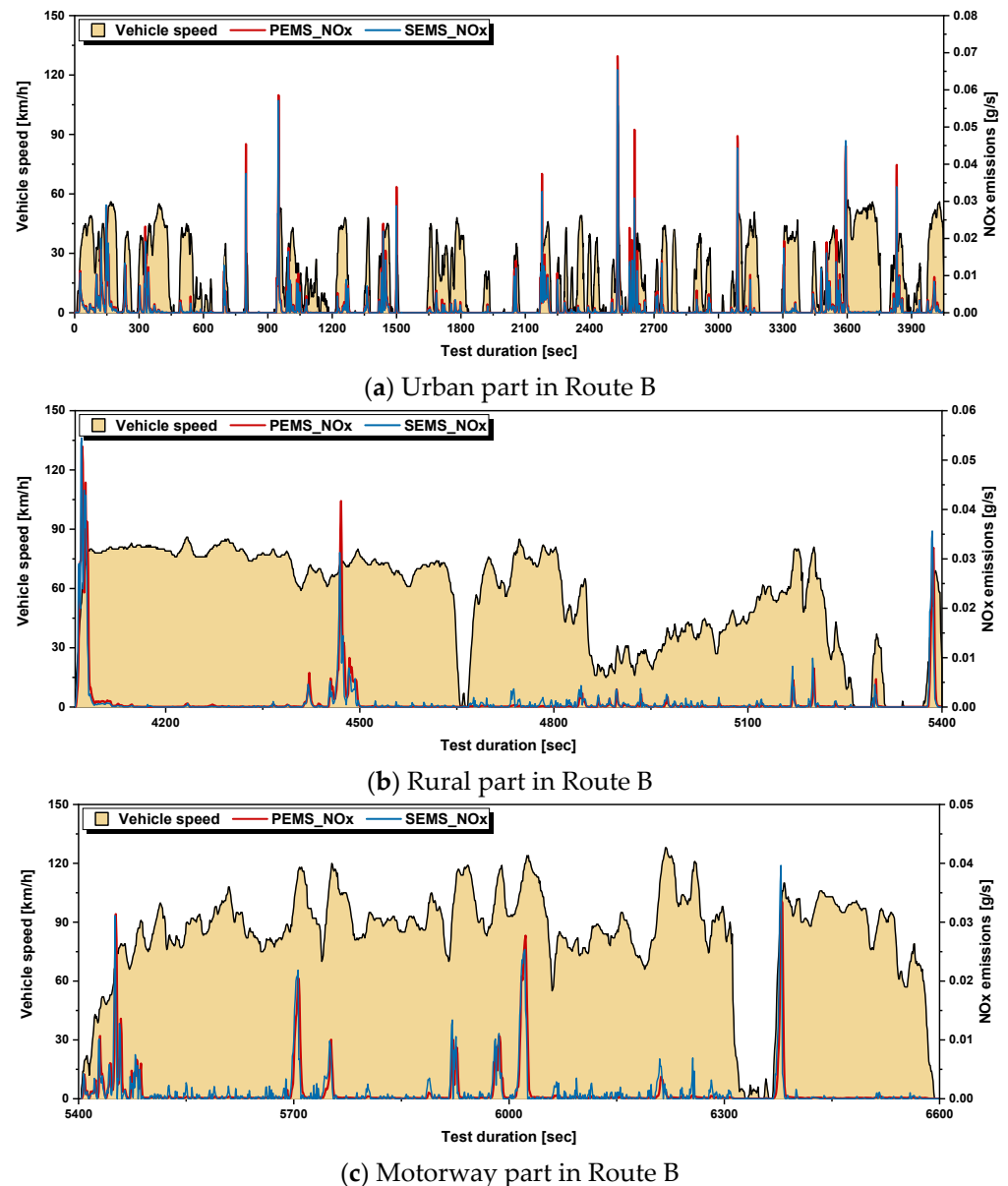


Figure 19. Real-time profiles of NO_x emissions measured by the PEMS and SEMS equipment under RDE Route B.

Figure 20 presents the difference between NO_x emissions measured by PEMS and SEMS equipment according to CO emissions in the urban part, under Routes A and B. Accordingly, it can be observed that the difference between NO_x emissions measured by PEMS and SEMS equipment was larger in Route B, where there are several stop durations.

Figure 21 presents the difference between NO_x emissions measured by PEMS and SEMS equipment according to the SCR efficiency under the motorway part in Routes A and B. According to the RDE tests, NO_x emissions abruptly increased in the section where vehicle speed was reduced, and then rapidly increased. Therefore, the SCR efficiency was reduced by this effect. This is believed to have triggered incomplete combustion, which is an inadequate air charge compared to the injected fuel quantity, owing to the delay in the increase in the rotational speed of the engine during rapid acceleration. Hence, NO_x emissions were increased by this effect. If significant amounts of NO_x emissions are released, it is believed that the SCR efficiency is reduced, owing to the relatively small amount of urea solution from the SCR system.

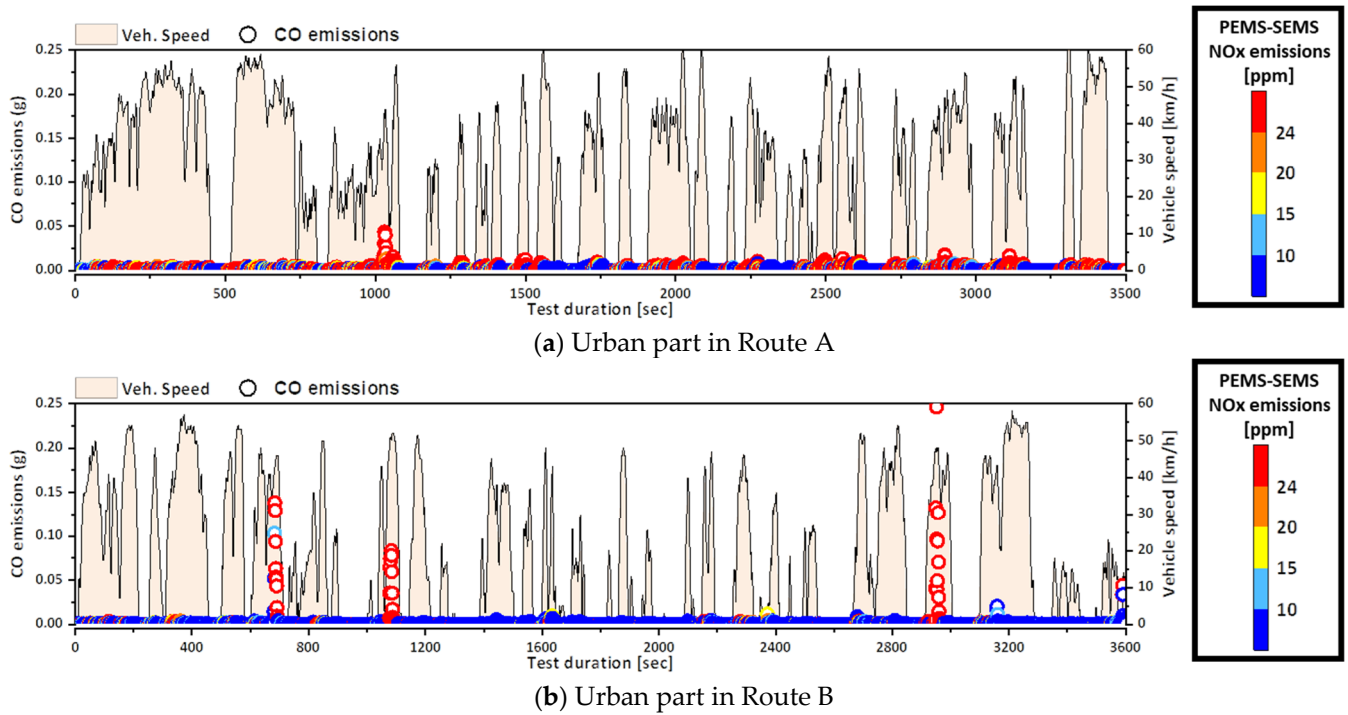


Figure 20. Real-time profiles of CO emissions and the difference between NOx emissions measured by the PEMS and SEMS equipment under urban part in Routes A and B.

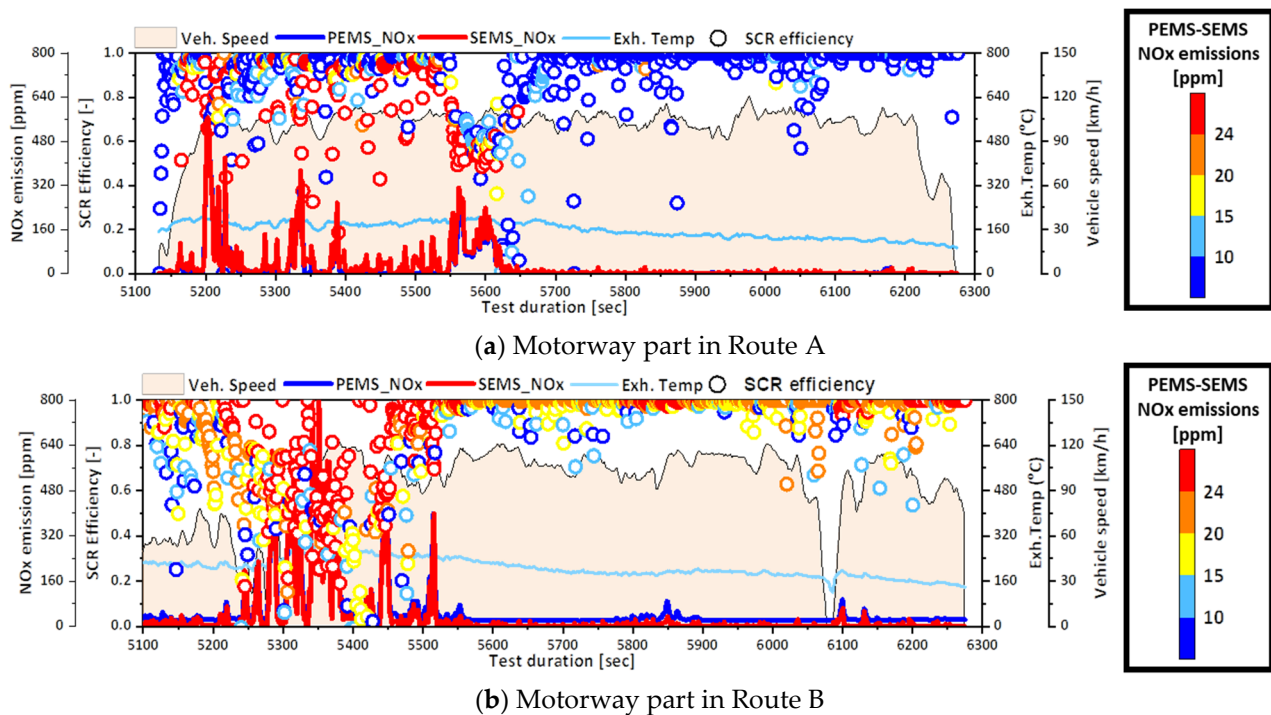


Figure 21. Real-time profiles of SCR efficiency and the difference between NOx emissions measured by the PEMS and SEMS equipment under motorway part in Routes A and B.

4. Conclusions

In this study, PEMS and SEMS equipment were installed on a test vehicle to simultaneously measure NOx emissions under various test modes in the laboratory and on

road. Based on these test results, the reliability of NO_x emissions measured by the SEMS equipment was verified as follows:

- The slope was significantly equal to 1, and the coefficient of determination was 0.93 or more when comparing between the vehicle speed and exhaust flow rate measured by the PEMS and SEMS equipment. It was possible to verify the reliability of the OBD data measured by the SEMS equipment.
- Via the correlation test results of PEMS and SEMS equipment in the laboratory, most of the NO_x emissions measured by the PEMS and SEMS equipment were within the current NO_x emission limit (0.08 g/km). It was verified that the slope of the NO_x emissions measured by the PEMS and SEMS equipment was significantly close to 1, and the coefficient of determination was 0.961, thus indicating that the results were highly similar.
- Regarding the on-road results of the PEMS and SEMS equipment obtained from the correlation tests, most of the test results were within the RDE NO_x emissions limit (0.1144 g/km). It was confirmed that the slope of the NO_x emissions measured by the PEMS and SEMS equipment was 0.816, which is lower than the slope obtained via the correlation test in the laboratory. In addition, the coefficient of determination was 0.922, thus indicating that the results were highly similar.
- However, NO_x emissions measured by the SEMS equipment were higher than those measured by the PEMS equipment under RDE tests. When NO_x emissions increase due to LNT regeneration and the SCR efficiency reduction, the SEMS equipment increases NO_x emissions by exceeding the limit of the O₂ measurement range.
- Finally, when comparing the two equipment types, the PEMS and SEMS equipment can be used interchangeably in the same way for measuring NO_x emissions. However, unlike the PEMS equipment, the SEMS equipment can measure NO emissions generated by urea solution. Therefore, it is necessary to install an additional NH₃ sensor for comparative analysis.

Author Contributions: Conceptualization, J.C. and M.S.C.; methodology, Y.S.Y.; validation, Y.S.Y.; J.W.J.; investigation, J.W.J.; data curation, Y.S.Y. and J.W.J.; writing—original draft preparation, Y.S.Y.; writing—review and editing, J.C.; supervision, J.C. and M.S.C.; funding acquisition, J.C. and M.S.C. All authors have read and agreed to the published version of the manuscript.

Funding: This research received no external funding.

Institutional Review Board Statement: No applicable.

Informed Consent Statement: Not applicable.

Data Availability Statement: The data of this study are available from the corresponding author upon reasonable request.

Acknowledgments: This research was supported by the Korea Evaluation Institute of Industrial Technology (20002762) and the National Research Foundation of Korea (NRF-2019R1I1A3A01062771).

Conflicts of Interest: The authors declare no conflict of interest.

References

1. Lee, D.I.; Yu, Y.S.; Chon, M.S.; Cha, J. A Study of Cold-start and Evaluation Method for Real Driving Emissions of Diesel Light-duty Vehicle. *Trans. Korean Soc. Automot. Eng.* **2019**, *27*, 199–206. [[CrossRef](#)]
2. Thompson, G.J.; Carder, D.K.; Besch, M.C.; Thiruvengadam, A.; Kappanna, H.K. *In-Use Emissions Testing of Light-Duty Diesel Vehicles in the United States*; West Virginia University: Morgantown, WV, USA, 2014.
3. Yu, Y.S.; Chon, M.S.; Cha, J. NO_x Characteristics of the Real Driving Emission with Data Calculation Methods. *Alex. Eng. J.* under review.
4. European Commission. *Amending Regulation (EC) No 692/2008 as Regards Emissions from Light Passenger and Commercial Vehicles (Euro 6)*; Regulation (EU) 2016/646; European Union: Luxembourg, 2016.
5. Vermeulen, R.J.; van Goethem, S.; Baarbe, H.L.; Zuidgeest, L.W.M.; Spreeen, J.S.; Vonk, W.A. SEMS operating as a proven system for screening real-world NO_x and NH₃ emissions. In Proceedings of the 20th International Transport and Air Pollution Conference, Graz, Austria, 18–19 September 2014; TAP paper 58.

6. Kadijk, G.; Vermeulen, R.J.; Buskermolen, E.G.; Elstgeest, M.; van Heesen, D.; Heijne, V.A.M.; Ligerink, N.E.; van der Mark, P.J. *NOx Emissions of Eighteen Diesel Light Commercial Vehicles: Results of the Dutch Light-Duty Road Vehicle Emission Testing Programme 2017*; TNO: The Hague, The Netherlands, 2017.
7. Kadijk, G.; Elstgeest, M.; Ligerink, N.E.; van der Mark, P.J. *Emissions of Twelve Petrol Vehicles with High Mileages*; TNO: The Hague, The Netherlands, 2018.
8. Sjödin, Å.; Borken-Kleefeld, J.; Carslaw, D.; Tate, J.; Alt, G.-M.; Fuente, J.D.; Bernard, Y.; Tietge, U.; McClintock, P.; Gentala, R.; et al. *Real-Driving Emissions from Diesel Passenger Cars Measured by Remote Sensing and as Compared with PEMS and Chassis Dynamometer Measurements—CONOX Task 2 Report*; IVL Swedish Environmental Research Institute: Stockholm, Sweden, 2018.
9. Lee, B.; Yun, B.; Jung, J.; Kim, D. Study on NOx Emission Characteristics of Diesel Light Duty Vehicles by Analyzing Massive Driving Data. *Trans. Korean Soc. Automot. Eng.* **2018**, *26*, 684–692. [[CrossRef](#)]
10. Yu, Y.S.; Jeong, J.W.; Kim, S.L.; Sim, I.; Chon, M.S.; Cha, J. A Study Correlations of NOx Emissions between PEMS and SEMS of Light-Duty Diesel Vehicle in Real Driving According to Ambient Temperature and Cold Start. *Trans. Korean Soc. Automot. Eng.* **2020**, *28*, 277–283. [[CrossRef](#)]
11. Yang, J.; Durbin, T.D.; Jiang, Y.; Tange, T.; Karavalakis, G.; Cocker, D.R.; Johnson, K.C. A comparison of a mini-PEMS and a 1065 compliant PEMS for on-road gaseous and particulate emissions from a light duty diesel truck. *Sci. Total Environ.* **2018**, *640–641*, 364–376. [[CrossRef](#)] [[PubMed](#)]
12. Vermeulen, R.J.; Ligerink, N.E.; Vonk, W.A.; Baarbe, H.L. A smart and robust NOx emission evaluation tool for the environmental screening of heavy-duty vehicles. In Proceedings of the 19th International Transport and Air Pollution Conference, Thessaloniki, Greece, 26–27 November 2012.
13. Ligerink, N.E.; Heijne, V.; Kadijk, G.; van der Mark, P.J.; Spreen, J.; Stelwagen, U. *NOx Emissions of Fifteen Euro 6 Diesel Cars: Results of the Dutch LD Road Vehicle Emission Testing Programme 2016*; TNO: The Hague, The Netherlands, 2016.
14. Heepen, F.; Weilin, Y. *SEMS for Individual Trip Reports and Long-Time Measurement*; SAE Technical Paper Series; SAE International: Warrendale, PA, USA, 2019.
15. Vermeulen, R.J.; van Gijlswijk, R.N.; van Goethem, S. NOx emissions of Heavy-Duty Vehicles with Euro VI Certified engines. In Proceedings of the Transport and Air Pollution Conference, Thessaloniki, Greece, 15–17 May 2019.
16. Ko, K.-H.; Choi, S.-C. A study on the improvement of vehicle fuel economy by fuel-cut driving. *J. Korea Acad. Ind. Coop. Soc.* **2012**, *13*, 498–503.
17. Sahner, K. Automotive Exhaust Gas Sensing—Current Trends. In Proceedings of the 14th International Meeting on Chemical Sensors—IMCS 2012, Nürnberg/Nuremberg, Germany, 20–23 May 2012; AMA-Science: Berlin, Germany, 2012.
18. Kato, N.; Nakagaki, K.; Ina, N. *Thick Film ZrO2 NOx Sensor*; SAE Technical Paper Series; SAE International: Warrendale, PA, USA, 1996.
19. Lee, D.I.; Yu, Y.S.; Park, J.; Chon, M.S.; Cha, J. NOx Conversion Efficiency of SCR Diesel Vehicle Under Cold Start Condition. *J. ILASS-Korea* **2018**, *23*, 244–253.
20. Bertoa, R.S.; Astorga, C. Impact of cold temperature on Euro 6 passenger car emissions. *Environ. Pollut.* **2018**, *234*, 318–329. [[CrossRef](#)] [[PubMed](#)]
21. Maurer, M.; Fortner, T.; Holler, P.; Zarl, S.; Eichlseder, H. Impact of cyclic lean-rich aging under DeSOx condition on the lean-gas light-off and hydrogen formation ability of a lean NOx trap (LNT). *Automot. Engine Technol.* **2017**, *2*, 63–77. [[CrossRef](#)]
22. Bari, S. Chapter 7: NOx Storage and Reduction for Diesel Engine Exhaust Aftertreatment. In *Diesel Engine: Combustion, Emissions and Condition Monitoring*; Bari, S., Ed.; IntechOpen: Adelaide, Australia, 2013; pp. 161–196.
23. Pereda-Ayo, B.; González-Velasco, J.R.; Burch, R.; Hardacre, C.; Chansai, S. Regeneration mechanism of a Lean NOx Trap (LNT) catalyst in the presence of NO investigated using isotope labelling techniques. *J. Catal.* **2012**, *285*, 177–186. [[CrossRef](#)]
24. Jang, W. Evaluation of Nitrogen Oxides (NOx) Emission and Its After-Treatment System Performance Characteristics from Diesel Passenger Vehicles on Real-World Driving with Ambient Temperature Effects. Ph.D. Thesis, Korea University, Seoul, Korea, February 2017.
25. Nova, I.; Tronconi, E. *Urea-SCR Technology for deNOx After Treatment of Diesel Exhausts*, 1st ed.; Springer: New York, NY, USA, 2014; pp. 1–716.
26. Fedoseev, G.; Loppolo, S.; Zhao, D.; Lamberts, T.; Linnartz, H. Low Temperature Surface Formation of NH3 and HNCO: Hydrogenation of nitrogen atoms in CO-rich interstellar ice analogues. *Mon. Not. R. Astron. Soc.* **2015**, *446*, 439–448. [[CrossRef](#)]
27. Gibbs, J.; Singh, G. *Innovative SCR Materials and Systems for Low Temperature Aftertreatment*, U.S. Annual Merit Review and Peer Evaluation Meeting (AMR); Department of Energy, Vehicle Technologies Office: Washington, DC, USA, 2017.
28. Jeong, J.W.; Sim, I.; Kim, S.L.; Yu, Y.S.; Chon, M.S.; Cha, J. A Correlation Analysis of NOx Emissions for Driving Condition between PEMS and SEMS Devices. *Trans. Korean Soc. Automot. Eng.* **2021**, *29*, 187–196. [[CrossRef](#)]
29. Aliramezani, M.; Koch, C.R.; Secanell, M.; Hayes, R.E.; Patrick, R. An electrochemical model of an amperometric NOx sensor. *Sens. Actuators B Chem.* **2019**, *290*, 302–311. [[CrossRef](#)]